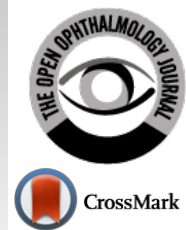




The Open Ophthalmology Journal

Content list available at: <https://openophthalmologyjournal.com>



RESEARCH ARTICLE

Photoacoustic Imaging of Enucleated Eyes from Patients with Uveal Melanoma can Reveal Extrascleral Growth

Ulf Dahlstrand^{1,*}, Aboma Merdasa¹, Jenny Hult¹, John Albinsson¹, Magnus Cinthio², Rafi Sheikh¹ and Malin Malmjö¹

¹Department of Clinical Sciences Lund, Ophthalmology, Lund University, Skåne University Hospital, Lund, Sweden

²Department of Biomedical Engineering, Faculty of Engineering, Lund University, Lund, Sweden

Abstract:

Background:

Uveal melanoma is treated by either enucleation (removal of the eye) or local eye-sparing therapies, depending on tumor size and whether there are signs of extrascleral growth. Photoacoustic (PA) imaging is a novel imaging modality that provides high-resolution images of the molecular composition of tissues.

Objective:

In this study, the feasibility of PA imaging for uveal melanomas and detection of extrascleral growth was explored.

Methods:

Seven enucleated human eyes with uveal melanomas were examined using PA imaging. The spectral signatures of the melanomas and the layers of the normal eyewall were characterized using 59 excitation wavelengths from 680 to 970 nm.

Results:

Significant differences were seen between the spectra obtained from melanoma and the healthy eyewall. Using spectral unmixing, melanin, hemoglobin and collagen could be mapped out, showing the architecture of the tumor in relation to the eyewall. This allowed visualization of regions where the tumor extended into the extrascleral space.

Conclusion:

PA imaging appears to have the potential to aid in assessing uveal melanomas and as a diagnostic tool for the detection of extrascleral growth.

Keywords: Enucleation, *Ex vivo*, Photoacoustic imaging, Spectral unmixing, Tumor, Uveal melanoma.

Article History

Received: July 17, 2021

Revised: October 6, 2021

Accepted: October 28, 2021

1. INTRODUCTION

Uveal melanoma is the most common primary ocular malignancy in adults and affects approximately 5 per million individuals per year [1]. It usually arises from the choroid (~85%), but can also originate in the ciliary body or the iris [2, 3]. Enucleation, where the eye is removed in its entirety, is the standard treatment for large tumors, recurring tumors, and when the probability of retaining vision is low. For smaller tumors, vision-sparing treatments are available, such as radiotherapy, including episcleral brachytherapy and stereotactic proton-beam therapy [3].

Extrascleral tumor extension, *i.e.*, when the tumor has spread through the wall of the eye (the sclera), is sometimes visible on macroscopic inspection or ultrasound examination. Otherwise, it may be discovered during surgery, once the sclera has been surgically exposed, or upon histopathological examination. It would thus be valuable to reveal extrascleral growth preoperatively in order to implement the optimal therapy [4]. There is a need for non-invasive diagnostic tools that can be used to map the extent of the tumor in detail, aiding the clinician in deciding which tumors are suitable for local, eye-sparing, treatment and cases where enucleation is necessary.

Uveal melanomas are traditionally examined with ultrasound, funduscopy, and fluorescein angiography. At

* Address correspondence to this author at the Department of Clinical Sciences Lund, Ophthalmology, Lund University, Skåne University Hospital, Lund, Ögonklinik A, Kioskgatan 1, Skåne University Hospital SE-221 85 Lund, Sweden; Tel: +4640331349; E-mail: ulf.dahlstrand@med.lu.se

ultrasound examination, a classic medium- to large-sized uveal melanoma appears as a dome- or mushroom-shaped choroidal mass with low or moderate internal reflectivity in A-mode. Smaller tumors and ciliary body tumors are more difficult to detect and pose a greater challenge to the clinician [5]. If the clinical situation is uncertain, invasive biopsies can be used, and although this does not appear to increase the risk of metastases [6], it is associated with potential side effects such as vitreous hemorrhage and retinal detachment [7].

Photoacoustic (PA) imaging, which combines the advantages of optical and ultrasound imaging, is one of the most promising emerging non-invasive bioimaging techniques [8]. A laser emits nanosecond pulses of light absorbed in the tissue, causing thermoelastic expansion detected by an ultrasound transducer. These ultrasonic waves are converted into a multispectral image of the tissue that provides information on its molecular composition. PA imaging thus provides more information than that on the anatomical features of the tissue, as in the case of ultrasound alone. It thus has the potential to help the clinician detect uveal melanoma at an early stage or in atypical cases.

PA imaging has mainly been used experimentally on animals, but in recent years human tissues and tumors have also been examined [9 - 12]. Very few studies have been carried out using PA imaging of human eyes [13, 14] and only one of uveal melanoma [15]. In the latter paper, only six laser wavelengths were used and the tumor borders were not assessed. The present study was therefore performed to investigate the feasibility of using PA imaging to detect uveal melanoma in enucleated eyes. Spectral unmixing was used to map the architecture of the melanoma, and the results were compared to histopathological findings. Particular attention was paid to extrascleral growth.

2. MATERIALS AND METHODS

2.1. Ethics

The experimental protocol was approved by the Ethics Committee at Lund University, Sweden, prior to the start of the study. The participants were given both verbal and written information about the study and its voluntary nature. Written consent was obtained from all subjects. The research adhered to the tenets of the Declaration of Helsinki as amended in 2013.

2.2. Patients

Seven patients undergoing enucleation were recruited from the Department of Ophthalmology at Skåne University Hospital in Lund, between November 2018 and November 2020. Four had been diagnosed with uveal melanoma that was too large for eye-sparing treatment. Three had previously been treated with brachytherapy and were now showing signs of recurrence. The median age at the time of surgery was 69 years. The characteristics of the patients and histological diagnosis of all the enucleated eyes are given in Table 1.

2.3. Surgery and Photoacoustic Examination

The eyes were enucleated under general anesthesia according to the standard clinical procedure. If there were any

signs of extrascleral growth preoperatively, on visual inspection or ultrasound, the conjunctiva and Tenon’s capsule of these regions were excised together with the eye. The optical nerve was cut, and the enucleated eye was immediately prepared for PA imaging. Prolene® 6-0 sutures (Ethicon, Somerville, NJ, USA) were attached at the insertion points of the medial and lateral recti muscles and two more were attached to the connective tissue surrounding the optical nerve. The eye was then mounted in a Perspex container filled with buffered saline solution using the four sutures. A layer of ultrasound-attenuating material was placed at the bottom of the container. The PA examination setup is shown in Fig. (1).

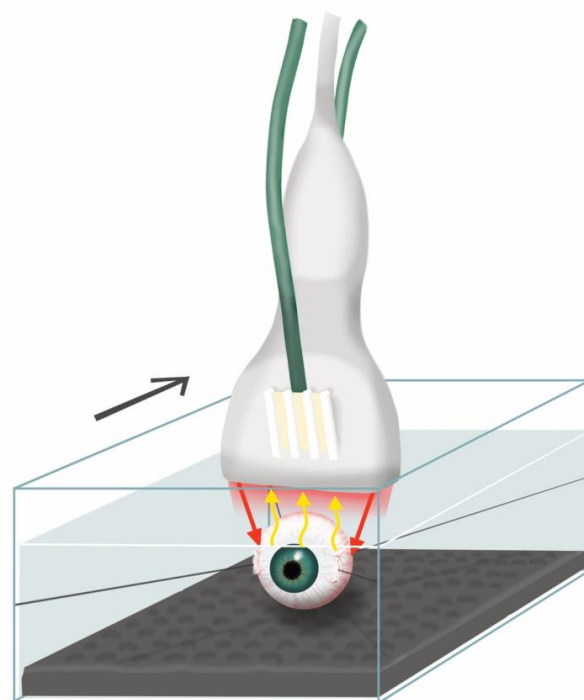


Fig. (1). Schematic illustration of the PA examination setup. The eye is mounted in a Perspex container filled with buffered saline solution using four sutures and scanned by PA imaging. The PA probe consists of an ultrasound probe with laser fiberoptic bundles attached. The tumor is irradiated with pulsed laser light (red) causing thermoelastic expansion, which in turn generates acoustic waves (yellow) that can be detected by a high-frequency ultrasound scanner.

Table 1. Characteristics of the patients and enucleated eyes.

Patient Number	Age at Surgery (y)	Sex	Eye Laterality	Previous Therapies	Origin	Cell Type	Extrascleral Growth
1	69	F	R	None	Choroid	Spindle	No
2	35	M	L	None	Ciliary body	Mixed	No
3	69	M	L	None	Choroid	Spindle	Yes
4	71	F	R	Brachytherapy	Choroid	Mixed	Yes
5	75	F	R	Brachytherapy	Choroid	Epithelioid	Yes
6	55	F	R	None	Choroid	Epithelioid	Yes
7	43	F	L	Brachytherapy + TTT	Choroid	Mixed	No

M = Male; F = Female; R = Right; L = Left; TTT = Transpupillary Thermotherapy; Extrascleral growth as defined by histopathological examination.

2.4. Photoacoustic System

A Vevo LAZR-X multimodal imaging system was used (FUJIFILM VisualSonics Inc., Toronto, ON, Canada), which allows examination using ultrahigh-frequency ultrasound and PA imaging. Diagnostic ultrasound is used as a guide during PA, and ultrasound images are interleaved with the laser pulses. The system has an ultrasound transducer and a fiberoptic bundle coupled to a 20-Hz tunable laser with a nanosecond pulse width. The laser was operated in the wavelength range 680 to 970 nm in intervals of 5 nm. Two planar light beams, located on either side of the ultrasound linear array, illuminate the eye. The PA waves were detected with a 25-MHz ultrasound linear array transducer (MX250, VisualSonics Inc.), which provides axial and lateral resolutions of 50 and 110 μm , respectively. A 10-mm-thick Aquaflex Ultrasound Gel Pad (Parker Laboratories Inc., Fairfield, NJ, USA) was used to ensure an adequate distance between the laser fibers and the eye. [REMOVED INCLUDEPICTURE FIELD] The PA transducer was mounted on an adjustable arm (Mounting Accessory, GCX Corporation, Petaluma, CA, USA) to avoid motion artifacts caused by the examiner and was driven by a stepping motor (VisualSonics Inc., Toronto, Canada). A single PA image was generated at every excitation wavelength, resulting in 59 PA images. When stacked together, these individual PA images generate one multispectral PA image where each pixel contains a single spectrum with 59 spectral components. The entire multispectral PA image is 512 pixels wide and 600-700 pixels high, resulting in 300 000 to 400 000 individual spectra.

2.5. Imaging of the Eye Wall and Melanoma

PA imaging was performed both over the healthy part of the eyewall and the part of the eyewall containing the tumor. When the enucleated eye was examined from the healthy side, light absorption in the melanin-rich choroid-retina complex made it impossible to obtain a sufficiently high photoacoustic signal from the tumor on the opposite side the eye, although it was visible with ultrasound. When the enucleated eye was examined from the tumor side, where the uveal melanoma was just below the sclera, it was possible to obtain a spectrum from the outer part of the tumor.

2.6. Spectral Unmixing

Spectral unmixing was performed on each individual PA spectrum. A linear unmixing model was employed using a non-negative least-squares fitting approach, according to Equation 1:

$$\mathbf{M} = \sum_{i=1}^N a_i \mathbf{S}_i + \mathbf{w} \quad (1)$$

where \mathbf{M} is a vector representing the measured spectrum, a_i the linear coefficients (or fractional abundances) of each endmember spectrum \mathbf{S}_i , and \mathbf{w} accounts for spectral noise. Endmember spectra representing oxygenated Hb (HbO_2), deoxygenated Hb (HbR), melanin and collagen were used in the unmixing model, from which the fractional abundance of each endmember spectrum was extracted. Images representing

the spatial distribution of each endmember can thereafter be superimposed on the ultrasound image in order to compare the structural information with the chromophore-specific information obtained from spectral unmixing. Using the spatially resolved images for the contribution of each end member on the pixel level, it is then possible to generate spatial averages anywhere in the images to visualize and compare changes in chromophore distributions. All analysis was performed in MATLAB R2018b (MathWorks Inc., Natick, MA, USA).

2.7. Histopathology

After *ex vivo* imaging, the eyes were placed in formalin and sent to the ophthalmic pathology laboratory at St. Erik Eye Hospital, Stockholm, Sweden, for histopathological examination, using standard staining with hematoxylin and eosin and Periodic acid-Schiff (PAS).

3. RESULTS

PA imaging of the healthy eye wall showed that the spectra obtained from regions within the sclera, the underlying choroid-retina complex, and the vitreous body from seven patients had distinctly different spectral shapes, as well as amplitudes (Fig. 2). Spectral unmixing was performed to identify the common constituents of the healthy parts of the eye, compared to those of the uveal melanoma (Fig. 3). In the healthy eyewall, the four endmember spectra representing HbO_2 , HbR , melanin, and collagen differed between the different layers. In the sclera, the PA spectrum was dominated by absorption by HbO_2 and collagen, while in the choroid-retina complex, the PA spectrum had a distinctly different shape and was dominated by melanin.

The PA spectrum from the melanoma differed from that of the healthy eyewall (Fig. 2), showing relatively higher levels of melanin, HbO_2 , and HbR (Fig. 3). Employing spectral unmixing enabled the architecture of the uveal melanoma to be mapped. Extrascleral growth identified in the histopathological examination was confirmed by PA imaging, using primarily the melanin signal as a marker (Fig. 4). Only the superficial part of the tumor could be mapped by PA imaging as most of the laser light was absorbed in the choroid-retina complex and the melanoma, allowing only a small fraction of the light to penetrate the deeper layers of the tumor.

4. DISCUSSION

PA imaging was used to characterize the photoacoustic properties of uveal melanoma in enucleated human eyes. Significant differences were seen between the spectra obtained from melanoma and the healthy eyewall. The tumors were clearly visible in the spectrally unmixed PA images due primarily to their high melanin content and high degree of vascularity. Only a few studies have been carried out previously using PA imaging to examine eyes [14, 16] and, to the best of our knowledge, only one study has been performed on patients with uveal melanoma [15]. Xu *et al.* examined five enucleated human eyes with uveal melanoma with PA imaging. The PA signal was consistent with a substantial amount of melanin in the tumors, which is in line with the findings of the

present study. However, the spectral resolution in the study by Xu *et al.* was low because of the use of only six laser wavelengths. In the present study, 59 wavelengths were used, to which spectral unmixing could be more reliably applied, allowing healthy tissue to be distinguished from tumor tissue. Two studies have been performed on animal eyes, but neither of these involved malignancies. De la Zerda *et al.* examined eyes from pigs and rabbits with a PA imaging system,

employing only two wavelengths [14]. They showed that the PA signal provided visualization of the blood vessels, which was difficult when using ultrasound alone. Kubelick *et al.* examined porcine eyes with PA imaging using the same wavelength range as in the present study, but in 10 nm steps [16]. They studied the anterior segment and mapped the melanin signal from brown and blue irises.

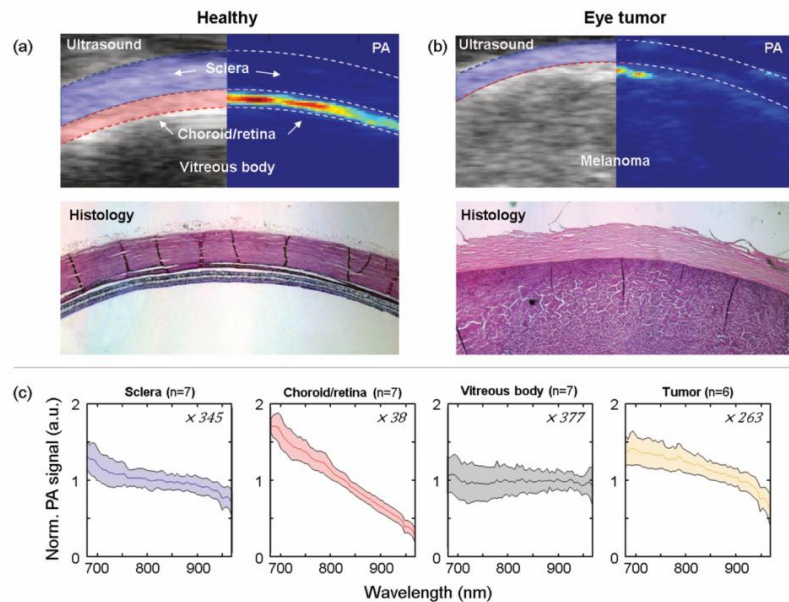


Fig. (2). Ultrasound and PA images as well as histological cross-sections of an enucleated eye, visualizing (a) the healthy eye wall and (b) a melanoma. (c) Graphs showing the mean PA spectra extracted from the sclera, choroid-retina complex, vitreous body, and tumor from the seven enucleated eyes (solid colored lines) together with one standard deviation (shaded colored areas). One tumor was excluded due to insufficient PA signal (patient 1). The number in each panel represents the normalization factor by which each spectrum was multiplied in order to have a mean amplitude of 1. Differences can be clearly seen between all spectra considering both shape and amplitude.

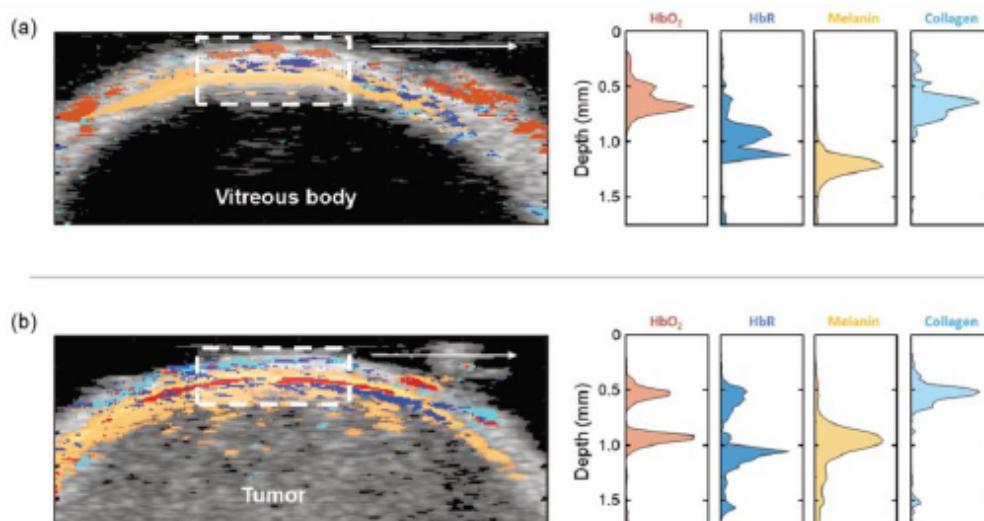


Fig. (3). PA images of a cross-section of (a) the healthy part of an eye wall and (b) an uveal melanoma. The contributions from the four endmembers (HbO₂, HbR, melanin, and collagen) obtained from PA imaging are superimposed on the ultrasound image. The graphs show the distribution of the spectral endmembers to a depth of 1.5 mm, represented as the spatial average, extracted for each horizontal line of pixels within the white dashed rectangles.

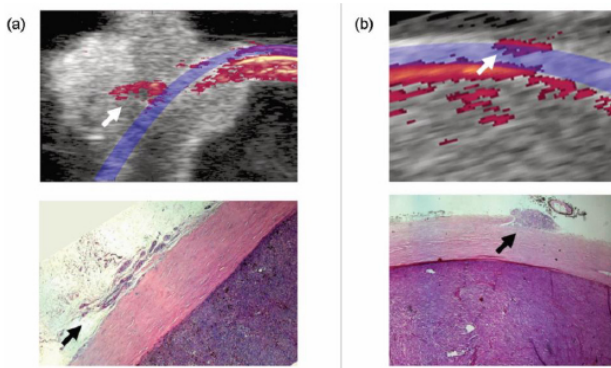


Fig. (4). Enucleated eyes from (a) patient number four and (b) patient number three that displayed uveal melanoma with extrascleral tumor growth (arrows) detected using spectral unmixing of multispectral PA images (above) and histology (below). The increased amount of melanin (red) in the melanoma is clearly visible in the PA images and is used to distinguish the tumor from the surrounding tissue and the sclera (blue). Histological examination of sections from the same regions confirm extrascleral tumor growth.

In the present study, PA imaging proved useful in mapping the architecture of melanoma and identifying cases of extrascleral growth. Extraocular uveal melanoma has a negative impact on patient survival and increases the risk of orbital recurrence [4]. Extrascleral growth is often suspected on visual inspection or ultrasound examination but is sometimes only confirmed during surgery or at histopathological examination. Other techniques that can be used to detect extrascleral growth are CT and MRI scanning, but these are not routinely performed preoperatively in cases of uveal melanoma, and may fail to detect small extrascleral tumor extensions [4]. In a small study by Récsán *et al.* MRI had a sensitivity and specificity of 100 and 89%, respectively, for detection of extrascleral extension [17]. Further, in 16 eyes with histopathological evidence of extrascleral extension, only 8 was detected with preoperative ocular ultrasound [18]. PA imaging provides a high-resolution image of the molecular composition of tissue, and thus offers unique possibilities to distinguish diseased tissue from healthy tissue.

In its current form, PA imaging cannot be used to examine eyes *in vivo* due to the risk of visual impairment resulting from the illuminating laser light. Light entering through the pupil risk being focused by the cornea and lens onto the retina, causing permanent retinal injuries. Even diffuse light, entering through the eyewall, where it is scattered and partly absorbed by the sclera and the choroid before reaching the retina, might cause thermal injuries, and this must be carefully studied before exploring the technique *in vivo*. However, PA imaging could possibly be implemented for the examination of eyes directly after enucleation to determine whether there is any extrascleral growth, removing the need to wait for the findings of histopathological examination. In some cases, this could mean that further tissue can be excised in the area of extended tumor growth to ensure radicality in the first surgery. This would reduce the number of surgeries required and the risk of recurrence.

Another benefit with the present study on PA imaging of

uveal melanoma, may be to pave the way for other spectroscopic techniques that could be used safely on eyes. Indeed, Krohn *et al.* used transscleral optical spectroscopy on nine enucleated human eyes, and found that sufficient light in the 400-1100 nm wavelength range penetrated the sclera and was transmitted back the spectrometer to be able to detect uveal melanoma on the inside. They found a correlation between the signal and the pigmentation grade of the tumor due to melanin being a strong chromophore in this wavelength range. The average tumor signal also indicated that there was more hemoglobin and less water than in the other, normal, side of the eye [19]. These results are in line with our findings of an increase in the signals from melanin and total hemoglobin in the tumor. As specific tumor characteristics, including the amount of melanin and vascularity, are known to correlate with patient prognosis in uveal melanoma, the PA technique also has potential to provide prognostic information [20, 21].

A limitation of the present study is that the PA signal does not penetrate very deep into the eye or the intraocular tumor. The choroid is a vascular structure immediately below the sclera, which constitutes the major blood supply to the outer retina. It also contains melanocytes, which play an important role in light absorption [22]. The presence of melanin in the choroid, as well as in the retinal pigment epithelium, helps to reduce undesirable intraocular scattering and reflection of light as it is a very strong absorber of light [23, 24]. As a result, only a small fraction of the excitation light reaches the layers below the choroid, resulting in low or no PA signal from deep intraocular structures.

Another limitation is leakage of a PA signal generated in regions not directly imaged, which also is a result of the strong light absorbing properties of the choroid and retinal pigment epithelium. As the eye is a spherical structure, the PA probe is not always perpendicular to the wall of the eye. The strong PA signals from the melanin-rich structures from adjacent areas, which also receive light, then leak into the measured image, appearing as additional structures. One way to circumvent this would be to rotate the eye underneath the probe in order to measure different sections, rather than moving the probe laterally.

It still remains to be explored whether uveal melanomas and uveal nevi, which also contain melanin, can be distinguished using PA imaging and spectral unmixing. Further studies are therefore needed to refine the technique, and examination of more enucleated eyes is required to determine whether it is possible to differentiate between different subtypes of uveal melanomas or to correlate the PA signal to prognostic biochemical features of the tumors.

CONCLUSION

In conclusion, multispectral PA imaging combined with spectral unmixing of enucleated eyes with uveal melanoma revealed the distribution of melanin, hemoglobin, and collagen, providing map of the overall architecture of the lesion. This revealed regions where the tumor extended through the sclera into the extrascleral space, making PA imaging a promising novel non-invasive method for assessing uveal melanomas in the future. PA imaging could be used for rapid intraoperative

determination of extrascleral growth to determine whether the excision is radical, or if further excision is necessary, saving time compared to conventional histopathological analysis. However, technical development is necessary before PA imaging can be used *in vivo* preoperatively due to the risk of retinal injury.

ETHICS APPROVAL AND CONSENT TO PARTICIPATE

The experimental was approved by the Ethics Committee at Lund University, Sweden, prior to the start of the study (2017/925).

HUMAN AND ANIMAL RIGHTS

No animals were used in this research. All human research procedures followed were in accordance with the ethical standards of the committee responsible for human experimentation (institutional and national), and with the Helsinki Declaration of 1975, as revised in 2013.

CONSENT FOR PUBLICATION

The participants were given both verbal and written information about the study and its voluntary nature. Written consent was obtained from all subjects.

AVAILABILITY OF DATA AND MATERIALS

Not applicable.

FUNDING

This study was supported by the Swedish Government Grant for Clinical Research (2018-0188; MM), Skåne University Hospital (SUS) Research Grants, Skåne County Council Research Grants, Lund University Grant for Research Infrastructure, the Swedish Cancer Foundation, Crown Princess Margaret's Foundation (KMA103; MM), Friends of the Visually Impaired Association in the county of Gävleborg (KMA), the Foundation for the Visually Impaired in the County of Malmöhus, Lund Laser Center Research Grant, IngaBritt and Arne Lundberg's Research Foundation and the Swedish Eye Foundation, Cronqvist Foundation, Swedish Medical Association and Lund University grant for Research Infrastructure.

CONFLICT OF INTEREST

The authors declare no conflict of interest, financial or otherwise.

ACKNOWLEDGEMENTS

The authors would like to thank Karl Engelsberg, Helen Sheppard and the surgical staff for valuable help with this project.

REFERENCES

- [1] McLaughlin CC, Wu XC, Jemal A, Martin HJ, Roche LM, Chen VW. Incidence of noncutaneous melanomas in the U.S. *Cancer* 2005; 103(5): 1000-7. [http://dx.doi.org/10.1002/ncr.20866] [PMID: 15651058]
- [2] Singh AD, Turell ME, Topham AK. Uveal melanoma: Trends in incidence, treatment, and survival. *Ophthalmology* 2011; 118(9): 1881-5. [http://dx.doi.org/10.1016/j.ophtha.2011.01.040] [PMID: 21704381]
- [3] Yang J, Manson DK, Marr BP, Carvajal RD. Carvajal, Treatment of uveal melanoma: Where are we now? *Ther Adv Med Oncol* 2018. 1758834018757175 eCollection
- [4] Blanco G. Diagnosis and treatment of orbital invasion in uveal melanoma. *Can J Ophthalmol* 2004; 39(4): 388-96. [http://dx.doi.org/10.1016/S0008-4182(04)80010-3] [PMID: 15327104]
- [5] Kivelä T. Diagnosis of uveal melanoma. *Dev Ophthalmol* 2012; 49: 1-15. [PMID: 22042009]
- [6] Bagger M, Smidt-Nielsen I, Andersen MK, *et al*. Long-term metastatic risk after biopsy of posterior uveal melanoma. *Ophthalmology* 2018; 125(12): 1969-76. [http://dx.doi.org/10.1016/j.ophtha.2018.03.047] [PMID: 29705056]
- [7] Finn AP, Materin MA, Mruthyunjaya P. Choroidal tumor biopsy: A review of the current state and a glance into future techniques. *Retina* 2018; 38(Suppl. 1): S79-87. [http://dx.doi.org/10.1097/IAE.0000000000001997] [PMID: 29280938]
- [8] Wang LV. Prospects of photoacoustic tomography. *Med Phys* 2008; 35(12): 5758-67. [http://dx.doi.org/10.1118/1.3013698] [PMID: 19175133]
- [9] Valluru KS, Willmann JK. Clinical photoacoustic imaging of cancer. *Ultrasonography* 2016; 35(4): 267-80. [http://dx.doi.org/10.14366/uscg.16035] [PMID: 27669961]
- [10] Valluru KS, Wilson KE, Willmann JK. Photoacoustic imaging in oncology: Translational preclinical and early clinical experience. *Radiology* 2016; 280(2): 332-49. [http://dx.doi.org/10.1148/radiol.16151414] [PMID: 27429141]
- [11] Dahlstrand U, Sheikh R, Merdasa A, *et al*. Photoacoustic imaging for three-dimensional visualization and delineation of basal cell carcinoma in patients. *Photoacoustics* 2020; 18 100187 eCollection
- [12] Hult J, Dahlstrand U, Merdasa A, *et al*. Unique spectral signature of human cutaneous squamous cell carcinoma by photoacoustic imaging. *J Biophotonics* 2020; 13(5): e201960212. [http://dx.doi.org/10.1002/jbio.201960212] [PMID: 32049420]
- [13] Liu W, Zhang HF. Photoacoustic imaging of the eye: A mini review. *Photoacoustics* 2016; 4(3): 112-23. [http://dx.doi.org/10.1016/j.pacs.2016.05.001] [PMID: 27761410]
- [14] de la Zerda A, Paulus YM, Teed R, *et al*. Photoacoustic ocular imaging. *Opt Lett* 2010; 35(3): 270-2. [http://dx.doi.org/10.1364/OL.35.000270] [PMID: 20125691]
- [15] Xu G, Xue Y, Özkurt ZG, *et al*. Photoacoustic imaging features of intraocular tumors: Retinoblastoma and uveal melanoma. *PLoS One* 2017; 12(2): e0170752. [http://dx.doi.org/10.1371/journal.pone.0170752] [PMID: 28231293]
- [16] Kubelick KP, Snider EJ, Ethier CR, Emelianov S. Photoacoustic properties of anterior ocular tissues. *J Biomed Opt* 2019; 24(5): 1-11. [http://dx.doi.org/10.1117/1.JBO.24.5.056004] [PMID: 31115200]
- [17] Récsán Z, Karlinger K, Fodor M, Zalatnai A, Papp M, Salacz G. MRI for the evaluation of scleral invasion and extrascleral extension of uveal melanomas. *Clin Radiol* 2002; 57(5): 371-6. [http://dx.doi.org/10.1053/crad.2001.0859] [PMID: 12014934]
- [18] Burris CKH, Papastefanou VP, Thaug C, *et al*. Detection of extrascleral extension in uveal melanoma with histopathological correlation. *Orbit* 2018; 37(4): 287-92. [http://dx.doi.org/10.1080/01676830.2017.1423083] [PMID: 29313397]
- [19] Krohn J, Svenmarker P, Xu CT, Mørk SJ, Andersson-Engels S. Transscleral optical spectroscopy of uveal melanoma in enucleated human eyes. *Invest Ophthalmol Vis Sci* 2012; 53(9): 5379-85. [http://dx.doi.org/10.1167/iovs.12-9840] [PMID: 22729436]
- [20] Brożyna AA, Józwicki W, Roszkowski K, Filipiak J, Słominski AT. Melanin content in melanoma metastases affects the outcome of radiotherapy. *Oncotarget* 2016; 7(14): 17844-53. [http://dx.doi.org/10.18632/oncotarget.7528] [PMID: 26910282]
- [21] Stålhammar G, See TRO, Phillips SS, Grossniklaus HE. Density of PAS positive patterns in uveal melanoma: Correlation with vasculogenic mimicry, gene expression class, BAP-1 expression, macrophage infiltration, and risk for metastasis. *Mol Vis* 2019; 25: 502-16. [PMID: 31588174]
- [22] Nickla DL, Wallman J. The multifunctional choroid. *Prog Retin Eye Res* 2010; 29(2): 144-68.

- [23] [http://dx.doi.org/10.1016/j.preteyeres.2009.12.002] [PMID: 20044062] Sarna T. Properties and function of the ocular melanin--a photobiophysical view. *J Photochem Photobiol B* 1992; 12(3): 215-58.
- [24] [http://dx.doi.org/10.1016/1011-1344(92)85027-R] [PMID: 1635010] Hu DN, Simon JD, Sarna T. Role of ocular melanin in ophthalmic physiology and pathology. *Photochem Photobiol* 2008; 84(3): 639-44. [http://dx.doi.org/10.1111/j.1751-1097.2008.00316.x] [PMID: 18346089]

© 2021 Dahlstrand *et al.*

This is an open access article distributed under the terms of the Creative Commons Attribution 4.0 International Public License (CC-BY 4.0), a copy of which is available at: <https://creativecommons.org/licenses/by/4.0/legalcode>. This license permits unrestricted use, distribution, and reproduction in any medium, provided the original author and source are credited.